Virulence factors analysis of native isolates of *Xanthomonas albilineans* and *Xanthomonas sacchari* from Tucumán, Argentina, reveals differences in pathogenic strategies

Natalia Mielnichuk[1], María Isabel Bianco[1], Pablo Marcelo Yaryura[2], Romina Priscila Bertani[3], Laila Toum[1], Yasmín Daglio[4], María Antonela Colonnella[5], Leonardo Lizarraga[5], Atilio Pedro Castagnaro[3] and Adrián Alberto Vojnov[1*]

[1]Instituto de Ciencia y Tecnología Dr. César Milstein, Fundación Pablo Cassará, CONICET, Saladillo 2468, Ciudad Autónoma de Buenos Aires, C1440FFX, Argentina

[2]Centro de Investigaciones y Transferencia de Villa María (CIT-VM), CONICET, Universidad Nacional de Villa María (UNVM), Villa María, Córdoba, Argentina

[3]Estación Experimental Agroindustrial Obispo Colombres. Av. William Cross 3150 (4101), Tucumán, Argentina.

[4]Centro de Investigación en Hidratos de Carbono (CIHIDECAR), CONICET, Universidad de Buenos Aires, Facultad de Ciencias Exactas y Naturales, Pabellón 2, Ciudad Autónoma de Buenos Aires, C1428EGA, Argentina.

[5]Centro de Investigaciones en Bionanociencias (CIBION-CONICET), Godoy Cruz 2390, 1st Floor, Ciudad Autónoma de Buenos Aires, C1425FQD, Argentina.

* Corresponding author: avojnov@centromilstein.org.ar

Running title: *X. albilineans* and *X. sacchari* pathogenic strategies

Keywords: *Xanthomonas,* sugarcane leaf scald, epiphytic, pathogen, biofilm, exopolysaccharide

ABSTRACT

Xanthomonas albilineans (*Xa*) and *Xanthomonas sacchari* (*Xs*) are both sugarcane pathogens. *Xa* is the causal agent of leaf scald disease, but there is limited information about *Xs* pathogenicity. The aim of this work was to study virulence factors of native strains of *Xa* (Xa32, Xa33 and XaM6) and *Xs* (Xs14 and Xs15) previously isolated from sugarcane with leaf scald symptoms to gain insight into the biology of each microorganism. We analyzed epiphytic survival, sensitivity to oxidative stress, extracellular degradative enzymes, cell motilities, exopolysaccharide (EPS) characteristics, cell adhesion, biofilm development and control of stomata regulation of the five strains. We observed that each species presented similar phenotypes for every factor analyzed. *Xa*

strains appeared to be more sensitive to oxidative stress and presented lower epiphytic survival than *Xs*. All strains presented endoglucanase activity, however we could only detect protease and amylase activities in *Xs* strains. Swimming and sliding were higher in *Xs*, but twitching was variable among species. We also observed that only *Xs* strains produced a xanthan-like EPS, presented a strong cell adhesion and structured biofilm. We detected some intraspecific variations showing that higher amounts of EPS produced by Xs14 correlated with its higher sliding motility and its homogenous and more adhesive biofilm. In addition, EPSs of Xs14 and Xs15 presented differences in strand height and acetyl percentage. Finally, we found that strains of both species were able to interfere with stomatal aperture mechanism. All these differences could influence the colonization strategies and/or disease progression in each species.

INTRODUCTION

The genus *Xanthomonas* involves several phytopathogenic species that can infect monocotyledonous and dicotyledonous crops. These bacteria can present an epiphytic phase on the leaf surface, where they move, attach and develop structures that protect them from environmental conditions. Later on, *Xanthomonas* spp. enter inside the plant through stomata, hydathodes and/or wounds depending on the species, and colonize different tissues. The infection outcome will range from a decreased in the crop production to the plant death (An *et al.*, 2019).

In particular, *Xanthomonas albilineans* (*Xa*) is a systemic vascular-invading pathogen that causes leaf scald disease in sugarcane (*Saccharum* spp.) (Rott and Davies, 2000). On the other hand, *Xanthomonas sacchari* (*Xs*), a phylogenetically close species to *Xa* (Young *et al.*, 2008), has recently been reported as the causal agent of sugarcane leaf chlorotic streak disease in China (Sun *et al.*, 2017). However, little is known about *Xs* biology, and no studies regarding the role of *Xs* virulence factors have been carried out besides *in silico* comparison with other *Xanthomonas* genomes including *Xa* (Pieretti *et al*., 2012). Indeed, several *Xs* strains have been studied showing some controversies regarding pathogenicity, host range and classification. For example, strain LMG476, isolated from diseased sugarcane, was first classified as *Xa*, then re-classified as *Xs* and recently included in a sequence comparative analysis against other *Xs* strains and closed related species of *Xa* (Pieretti *et al.*, 2015). Strain NCPPB4303 was isolated from an insect on a diseased

banana plant (Studholme *et al.*, 2011) and strain R1 was described as a biocontrol bacterium isolated from rice seed (Fang *et al.*, 2015). In line with these controversies, in this work we characterized native strains of *Xs* along with native strains of *Xa* that were all previously isolated from sugarcane with leaf scald disease symptoms.

Leaf scald is one of the major worldwide diseases that affect sugarcane. The disease can cause cane tonnage losses and juice quality reduction in susceptible varieties. Although it is mainly controlled by the used of resistant varieties, still new outbreaks are reported (Lin *et al.*, 2018; Ntambo *et al.*, 2019). Symptoms vary from a single white stripe parallel to the main veins ('pencil-line') to complete wilting and necrosis of infected leaves leading to plant death. The disease may present a latent phase when the pathogen remains undetected for several months in symptomless plants. This scenario makes difficult diagnosis and allows the spread of the pathogen. Certainly, leaf scald is mainly transmitted mechanically by knives and harvesters and by planting infected setts (Rott and Davies, 2000). Nevertheless, some authors demonstrated the contribution of aerial transmission and epiphytic populations on the disease cycle suggesting stomata as the main entrance of epiphytic *Xa* to the plant (Champoiseau *et al.*, 2009; Daugrois *et al.*, 2012; Mensi *et al.*, 2016). Once inside sugarcane, *Xa* lives mostly in the xylem, although it can also be in contact with parenchyma cells (Mensi *et al.*, 2014). Xylem presents particular features: it is a water transport network of vessels composed of dead, lignified cells. And xylem sap, rich in cell-wall breakdown products, would be the only nutrient source available. *In silico* studies suggested that *Xa* presents certain adaptations, such as specialized degradative enzymes and transporters, supporting the concept that *Xa* consumes cell-wall derived sugars (Pieretti *et al.*, 2012).

It is well known that *Xanthomonas* spp. exert different virulence factors such as the secretion of a wide range of enzymes, different types of cell motilities, secretion of exopolysaccharide (EPS), cell adhesion and biofilm formation (Büttner and Bonas, 2010). Some of these virulence factors influence each other during the disease progress. For instance, degradative enzymes fight plant defenses, enhance pathogen motility and facilitate acquisition of nutrients (Pfeilmeier *et al.*, 2016). Furthermore, cell motilities like swimming (flagella-dependent) and twitching (flagella-independent) affect cell adhesion and biofilm development (An *et al.*, 2019). Comparative genomic studies revealed that most of the known virulence factors described in other *Xanthomonas* spp. are present in *Xa*, except for the hypersensitive response and pathogenicity (Hrp) type III secretion system (T3SS) and the *gum* gene cluster (Pieretti *et al.*, 2012). T3SS Hrp

system is a syringe-like apparatus that delivers proteins (Hrp type III effectors) to the host cell (An *et al.* 2019). *Xa* lacks the structural components as well as known Hrp type III associated effectors (Pieretti *et al.*, 2012). In the case of *Xs*, the *gum* gene cluster is present, but it also lacks the T3SS Hrp system (Studholme *et al.*, 2011).

Specifically, the *gum* gene cluster consists of 12 genes (*gumB* to *gumM*) that allow the biosynthesis, polymerization, substitution and exportation of xanthan (Becker *et al.*, 1998). Xanthan is the main EPS produce by most *Xanthomonas* spp. and it is a key virulence factor of these bacteria. It protects xanthomonads from adverse environments contributing to epiphytic survival and can interfere with plant defense by suppressing callose deposition and regulating stomata aperture (An *et al.*, 2019). Moreover, xanthan is necessary for biofilm formation (Bütner and Bonas, 2010). Biofilm enclosed and protect *Xanthomonas* spp. from environmental stresses, host defense mechanisms and antimicrobial compounds, therefore being associated with epiphytic survival and virulence (Büttner and Bonas, 2010).

As mentioned above, *Xs* has the *gum* gene cluster; thus, it is probable that it synthesizes xanthan. However, until now, there are no reports about the characteristics of the EPS produced by *Xs*. Xanthan is composed of penta-saccharide repeating units, formed by a cellulose backbone with a side chain of an inner mannose, a glucuronic acid and a terminal mannose. Non-glycosidic substitutes can be linked to the inner mannose (acetyl groups) or to the terminal mannose (acetyl or ketal-pyruvate groups) (Becker *et al.*, 1998). The nature and degree of substitutions influence the structure of xanthan leading to effects on its role as virulence factor (Bianco *et al.*, 2016; Conforte *et al.*, 2019).

To our knowledge, in Argentina, previous reports have focused on the description of the leaf scald symptomatology, diagnosis, selection and development of sugarcane varieties resistant to *Xa* (Filippone *et al.*, 2010; Noguera *et al.*, 2014). Nevertheless, there are no research works about virulence factors of native strains of this phytopathogen, bringing up the importance of studying native isolates due to known diversity of *Xa* (Zhang *et al.*, 2020). Additionally, the presence of both *Xa* and *Xs* in sugarcane with leaf scald disease rise the question of the co existence of both bacteria in sugarcane fields, and whether they occupy the same niche inside the plant. Finally, there is no knowledge of the pathogenic strategy or virulence factors used by *Xs*. Therefore, the aim of this work was to investigate virulence factors of native strains of both species found in sugarcane with leaf scald disease symptoms in Tucumán, Argentina. We studied the epiphytic survival and early steps of disease progress through measurements of oxidative stress sensitivity,

production of extracellular enzymes, cell motility, EPS production, cell adhesion and biofilm formation. The ability to interfere with stomata aperture regulation in plant was also analyzed. This is the first step to address the pathogen strategies implemented by these two species as well as to understand in the future the possible association of both microorganisms with sugarcane plants.

MATERIALS AND METHODS

Bacterial strains and growth conditions

Bacteria used in this work belong to a collection kindly donated by the Estación Experimental Agroindustrial Obispo Colombres (EEAOC-Tucumán, Argentina). This collection includes unidentified bacteria isolated from leaves of sugarcane plants with leaf scald symptoms in fields of Tucumán, NW Argentina.

Xa and *Xs* strains were grown at 28ºC using shaking at 200 rpm in modified Wilbrink's (MW) medium (Rott *et al*., 2013) containing 1% (w/v) sucrose, 0.5% (w/v) peptone, 0.05% (w/v) $K_2HPO_4 \bullet 3H_2O$, 0.025% (w/v) $MgSO_4 \bullet 7H_2O$, 0.005% (w/v) Na_2SO_3, pH 6.8 to 7.0, and 1.5% (w/v) agar for solid medium; or Y minimal medium (YMM) (Malamud *et al*., 2011) containing 0.001% (w/v) $MgSO_4 \bullet 7H_2O$, 0.0022% (w/v) $CaCl_2 \bullet 75H_2O$, 0.0022% (w/v) $K_2HPO_4 \bullet 3H_2O$, 0.0002% (w/v) $FeCl_3$ salts, supplemented with 1% (w/v) sucrose, 0.11% (w/v) glutamate and 0.3% (w/v) cassaminoacids or 0.11% (w/v) glutamate and 1% (w/v) glucose when indicated. *Escherichia coli* S17-1 was grown at 37ºC in Luria-Bertani medium. When required, the antibiotics cephalexin (50 µg/ml) or kanamycin (100 µg/ml) were added to the growth media.

Bacteria genotypic identification

Bacterial genomic DNA was extracted according to Aljanabi *et al*. (1999). We used diagnosis leaf scald disease primers PGLB1 and PGLB2 (Pan *et al.*, 1999) to amplify a 288 pb fragment of the 16S-23S ribosomal DNA ITS specific of *Xa*. PCR amplification of the 16S rRNA gene was performed using universal primers 27F and 1492R (Lane, 1991). Amplicons were sequenced (Macrogen Inc. Seoul, South Korea) using the same set of primers to determine bacteria identities. Sequence analysis was performed using the BLASTn tool in the National Center for Biotechnology Institute (NCBI) website (https://blast.ncbi.nlm.nih.gov/Blast.cgi). We deposited the 16S rDNA sequences of strains Xs14, Xs15, Xa32, Xa33 and XaM6 (see Results) and the 288 pb sequence of the 16S-23S rDNA ITS corresponding to strains Xs14 and Xa33 (MT904291 and

MT904290 respectively) at the NCBI GenBank genome database (NCBI, Bethesda, MD). Primers are listed in Table S1.

Bacterial epiphytic survival

We assessed *Xa* and *Xs* epiphytic survival using the sugarcane variety TUC 97-8 (moderately susceptible to *Xa*). For this, four to five week-old plants grown from stalks were foliar sprayed until dripping with bacterial suspensions of Xs14, Xs15, Xa32, Xa33 and XaM6 adjusted to OD_{600} 0.1 (~ 1×10^8 CFU/ml) in 10 mM $MgCl_2$ containing Silwet-L77 0.05%. We performed the experiment under controlled conditions of photoperiod and temperature (12-h-light and 12-h-dark cycle at 25 to 28ºC). The negative control consisted in sugarcane plants treated with 10 mM $MgCl_2$ solution supplemented with 0.05% Silwet-L77. Three plants were used per treatment. To evaluate the epiphytic survival of *Xa* and *Xs* strains, a leaf area of 3 cm^2 was cut from a random leaf of each replicate at 0, 2, 4, 6, 8, 10, 12 and 16 days post inoculation. Samples were gently vortexed in 1 ml of 10 mM $MgCl_2$ and bacterial growth was quantified by dilution plating on MW agar medium. Plates were incubated at 28ºC and colonies counted after 48-72 h. Population data were calculated as $\log_{10}$ (CFU/cm^2). The experiment was done three times.

Oxidative stress sensitivity assay

For each strain tested, 100 µl of an overnight culture grown in liquid MW medium was spread on MW agar plates. We placed Whatman paper discs embedded with 5 µl of either 100 mM or 400 mM H_2O_2 over the MW agar plates. Sensitivity to H_2O_2 was calculated as the area of growth inhibition around the paper disc after 48 h at 28°C using ImageJ software (https://imagej.nih.gov/ij/). Four replicates were carried out per assay in two independent experiments.

Extracellular degradative enzymes assay

We measured enzyme activities by radial diffusion assays in substrate containing agar plates using 10 µl of cell free supernatants obtained from overnight cultures. Indicator plates for endoglucanase, protease and amylase activities contained agar 1.5% (w/v) and were supplemented with 0.125% (w/v) carboxymethylcellulose (CMC), 1% (w/v) skimmed milk or 1% (w/v) starch respectively. In all cases, degradation halos (diameter of the clear zone around the cell free

supernatants) were developed after 24 h at 28ºC. For CMC, plates were incubated with an aqueous Congo red 0.1% (w/v) solution for 30 min, followed by 3 washes with NaCl 5 M. Starch degradation was developed with Lugol solution. Finally, protease activity was detected by eye. Degradation halos were measured using the ImageJ software. Three independent experiments were performed in triplicates.

Swimming, sliding and twitching motility assays

Swimming and sliding assays were performed as described before (Malamud *et al.*, 2011; Rott *et al.*, 2013). Briefly, strains were grown overnight in liquid MW medium. Then 4µl of bacterial cultures adjusted to OD_{600} 0.1 were inoculated on top of the agar medium for sliding or stab-inoculated using a pipette to the bottom of the Petri dish for swimming assays. We evaluated swimming motility on MW medium containing 0.25% (w/v) agar, and sliding on MW medium using 0.5% (w/v) agar. All plates were incubated at 28ºC for 72 h and bacteria motility was measured as the colony outer halo. Experiments were performed three times, with triplicates each one. Twitching motility was estimated by microscope observation of the edge of the colony stained with 0.1% (w/v) crystal violet (CV) (Felipe *et al.*, 2018).

Exopolysaccharide (EPS) production and characterization

For EPS production, strains were grown for 48 h in liquid MW medium supplemented with 2% (w/v) sucrose, unless indicated otherwise. Cells were removed by centrifugation (25000 *g* for 2 h) and EPSs were precipitated using 1% (w/v) KCl and 2 volumes of ethanol. EPSs were collected and dried at room temperature (RT). The amount of EPS produced by each strain was measured in grams, relativized to the bacterial growth expressed as $\log_{10}$ (CFU/ml).

In order to characterize the EPSs, we analyzed the viscosity, macroscopic and microscopy appearance, and chemical composition of the EPS produced by each strain.

The viscosity was measured as the low shear rate viscosity (LSRV) for a 0.45% EPS solution in synthetic tap water (16.2 mM NaCl, 0.95 mM $CaCl_2$) at RT using a Brookfield viscometer (RVTD II) with spindle Nº 1 at 3 rpm.

To study the microscopic aspect of EPS strands, we analyzed an aqueous suspension of EPS by atomic force microscopy (AFM). AFM samples were prepared by spin coating. A volume 5 µl of each sample of 1µg/ml was deposited over Muscovite mica discs grade V1 (Ted Pella) of 10 mm diameter previously cleaved. Sample drop over mica discs was left for 1 min to promote

interactions with the substrate. Then, mica disc was accelerated up to a rotation speed of 2000 rpm, and finally the rotation speed was constant for 2.50 min at 2000 rpm. AFM imaging was performed on a MultiMode 8 equipped with a Nanoscope V controller (Bruker, Santa Barbara, CA, USA). AFM images were acquired using tapping mode. Silicon nitride cantilever with a nominal spring constant of 40 N/m and a nominal resonance frequency of ~320 kHz (NCHV, Bruker AFM Probes, Santa Barbara, CA, USA) were employed. The images were acquired at a resolution of 512 pixels and analyzed using Gwyddion version 2.46 software (Brno, Czech Republic). The images were flattened applying the following tools: align rows, remove scars and flatten base. Strand detection was performed by thresholding and filtering. The height mean value of EPS strands, which is the mean of all height values occurring inside the chain, was taken. This set of values was used as the parameter for a statistical analysis to perform boxplot graphs.

For the purpose of analyzing EPS chemical composition, the neutral monosaccharide molar percentage was determined by gas liquid chromatography (GLC) after hydrolysis with 2 M trifluoroacetic acid. GLC was carried out on a Hewlett–Packard 5890A gas-liquid chromatograph equipped with a flame ionization detector and fitted with a fused silica column (0.25 mm id × 30 m) WCOT-coated with a 0.20 μm film of SP-2330. Assignments were referred to a mixture of standard alditol acetates. When necessary, GLC–mass spectrometry (MS) analyses were carried out on a Shimadzu QP 5050 A (Kyoto, Japan) apparatus. Uronic acids were dosed according to Filisetti-Cozzi and Carpita (1991) referring to glucuronolactone as standard. Pyruvic acid was determined by the method of Koepsell and Sharpe (as described in Conforte *et al*., 2019) and the quantification of acetyl groups according to Hestrin (as described in Conforte *et al*., 2019) using acetylcholine as standard.

Detection of *X. sacchari gum* operon genes

In order to check the presence or absence of biosynthetic *gum* genes in the genomes of *Xs* strains, specific primers for *gumB*, *gumC*, *gumD*, *gumE*, *gumF*, *gumH*, *gumI*, *gumK*, *gumL* and *gumM* were designed based on the genomic sequence of *X. sacchari* R1 (https://www.ncbi.nlm.nih.gov/nuccore/743685209). A standard PCR, using 55°C annealing temperature and 30 cycles program was performed using genomic DNA as template (Primers are listed in Table S1).

Bacterial adhesion assay

Bacterial adhesion to abiotic surfaces was investigated using the CV technique (O'Toole and Kolter, 1998) in a 96-well microtiter polystyrene plate. Briefly, bacterial strains were grown overnight in liquid MW medium and inoculated into YMM supplemented with 1% (w/v) sucrose, 0.11% (w/v) glutamate and 0.3% (w/v) cassaminoacids. Aliquots of 200 µl of each bacterial suspension (OD_{600} 0.1) were used per well, and microplates were incubated at 28ºC for 48 h with no agitation. After this time, media was gently removed, and wells were washed twice with 0.9% (w/v) NaCl and air-dried. Then, each well was stained using 0.1% (w/v) CV solution in water for 30 min at RT. Finally, the unbound CV was washed twice with 0.9% (w/v) NaCl and wells were air-dried. CV was dissolved by adding 200 µl of ethanol:acetone solution (80:20 v/v) to each well. After 10 min of incubation at RT with gentle agitation, absorbance was measured at 570 nm (CV_{570}). The adhesion value was normalized to the number of non-adhere cells at OD_{600} (CV_{570}/OD_{600}). The experiment was performed three times with 10 replicates per treatment.

Biofilm formation analyzed by confocal laser scanning microscopy (CLSM)

To study biofilm development, *Xa* and *Xs* strains were transformed by conjugation using *E. coli* S17-1 carrying the pBBR2-GFP plasmid (Bianco *et al*., 2016). For biofilm experiments, strain aliquots of 500 µl were grown at 28ºC in a chambered cover-glass slide containing a 1-mm- thick borosilicate glass, as previously described (Malamud *et al*. 2011). Initial OD_{600} was set at 0.0002 in YMM supplemented with 1% (w/v) sucrose, 0.11% (w/v) glutamate and 0.3% (w/v) cassaminoacids. Biofilm formation was monitored with an inverted microscope Nikon Eclipse TE 2000-E2 CLSM (Nikon, Melville, NY, USA) every 24 h up to a maximum period of 5 days. Here we show images for 48, 72 and 96 h. Three-dimensional images were generated with IMARIS 6.3.1 software (Bitplane, St. Paul, MN, USA) and, subsequently, were analyzed using COMSTAT 2.1 Software Image Processing Toolbox, as previously described (Bianco *et al*., 2016). Images of two independent experiments were analyzed.

Stomatal aperture bioassays

Stomatal bioassays were performed as previously described (Bianco *et al.*, 2016). For all experiments, epidermal abaxial peels from leaves of four week-old plants were floated in 10:10 buffer (10 mM KCl and 10 mM MES-KOH, pH 6.15) under light for 2 h. For bacterial assays, cultures were washed and resuspended in buffer 10:10 with OD_{600} adjusted to 0.5 (~ 5×10^8 CFU/ml). Stomatal measurements were performed after 1 and 3 h of incubation with the bacterial

suspension. For microbe associated molecular pattern (MAMP) response experiments, peels were incubated using 200 µg/ml EPS for 1 h. After this time, 5 µM flg22 (flagellin derived 22-aminoacid peptide) was added to the medium and peels were incubated for another 1.5 h. We measured stomata aperture at 400x. Data are presented as the mean from 80 measurements, collected from two independent experiments.

Statistical analysis

Statistical analysis was performed using GraphPad Prism 6 software (https://www.graphpad.com/scientific-software/prism/). One-way ANOVA (*post hoc* Tukey´s test), two-way ANOVA (*post hoc* Sidak´s or Tukey´s test), Student´s *t* or Mann-Whitney tests were used. In all cases, significance level was set at $P < 0.05$. Data of all experiments are expressed as mean ± the standard error of the mean (SEM); except for EPS strand mean height that is expressed as median with data range.

RESULTS

Identification of *Xanthomonas* strains

Aiming to identify *Xa* native strains, we analyzed 23 isolates from a bacteria collection donated by the EEAOC using specific diagnosis primers for leaf scald disease that amplify a fragment of the 16S-23S rDNA ITS of *Xa* genomic DNA (Pan *et al.*, 1999). We found five isolates that were PCR positive: 14, 15, 32, 33 and M6. However, when the 16S rRNA gene was sequenced, only three isolates were confirmed as *Xa*: strains named Xa32, Xa33 and XaM6 (annotated as GenBank Accession Nº MT802169, MT802170 and MT802171 respectively). The other two isolates were identified as *Xs*: strains named Xs14 and Xs15 (annotated as GenBank Accession Nº MT802172 and MT802173 respectively). Considering that *Xs* was recently reported as a sugarcane pathogen (Sun *et al*., 2017), we included Xs14 and Xs15, along with Xa32, Xa33 and XaM6 strains in this study.

Differences in epiphytic survival between *Xa* and *Xs* strains

To understand possible differences between the two species lifestyle, we first investigated the epiphytic survival of the five strains (Xs14, Xs15, Xa32, Xa33 and XaM6). For that, we monitored the number of bacterial cells present on the leaf surface of sugarcane over a period of 16 days. Figure 1 shows that bacterial populations of *Xs* survived longer than those of *Xa*. Both Xs14 and

Xs15 presented a significantly higher cell population than all three *Xa* strains at 10 days post inoculation (dpi). The difference in survival began at 8 dpi, when Xs14 population was already significantly higher than Xa33 and XaM6, and Xs15 higher than XaM6. We observed that population size of *Xs* strains initially increased about 100 times, and then each strain declined with different rates: for Xs14 there was a decreased followed by a stabilization of the population size up to 10 dpi and then a sharp decline; while for Xs15 there was a constant decline from 2 dpi up to 12 dpi (Figure 1a). On the other hand, *Xa* presented a different pattern. At 2 dpi the population size of Xa32 and Xa33 increased about 10 times and then it was unchanged until 6 dpi. Similarly, XaM6 survival did not decline until 6 dpi although this strain did not present the initial increase. For this reason, XaM6 values were always below those for Xa32 and Xa33. All three populations sizes declined sharply, but with different rates, between 6 dpi and 10 dpi (Figure 1b).

Sensitivity to oxidative stress

To test if the differences in epiphytic survival among the five strains were due, in part, to differential response to environmental stress conditions, the effect of oxidative stress on bacterial survival was analyzed. To do that, we assessed the sensitivity of each strain to reactive oxygen species using different concentrations of H_2O_2 as stressor agent. While 100 mM of H_2O_2 already produced an area of growth inhibition for *Xa* strains (~ 1.4 cm^2), *Xs* strains were insensitive to this concentration (Figure 2a). In addition, *Xa* strains were significantly more sensitive than *Xs* strains to 400 mM of H_2O_2 showing a twenty fold difference between the averages of the area of growth inhibition of each species (~ 0.2 cm^2 vs. ~ 4.25 cm^2) (Figure 2a).

Production of degradative extracellular enzymes

As mentioned before, *Xanthomonas* spp. secret a wide range of enzymatic activities that contributes to disease progress. Among this battery of enzymes we analyzed the production of extracellular endoglucanase, protease and amylase. As it can be seen in Figure 2b, both *Xs* strains showed significantly higher levels of all activities tested. The endoglucanase activity of *Xa* strains was much lower when compared to *Xs* strains (19%/Xa32; 10%/Xa33; 49%/XaM6) (Figure 2b left panel). The difference was more striking when extracellular protease and amylase were analyzed since no activity was detected in any of the *Xa* strains (Figure 2b central and right panel). Interestingly Xs14 presented significant higher activity levels of protease and amylase than Xs15.

Cell motility displayed by *Xa* and *Xs* strains

Since cell motility is related to migration on the plant surface and inside the host tissue, we characterized the ability of the five strains to move through sliding, swimming and twitching. *Xs* strains showed significant higher sliding and swimming motilities than *Xa* strains, measured as the colony growth halo (Figure 3 top and middle panel). In particular, while all *Xa* strains exhibited similar very low sliding motility, Xs14 showed a value of sliding three times higher than Xs15. Conversely, swimming of Xs15 was significantly higher than swimming of Xs14. All *Xa* strains presented again significantly lower motility than *Xs* although this time some differences among the *Xa* strains were detected.

In contrast, twitching motility did not correlate with species and only Xs15, Xa32 and Xa33 presented the characteristic non-linear edge of the colony interrupted by budding, indicative of the spreading morphology in twitching. Xs14 and XaM6 showed colonies with smooth, whole or slightly wavy edges, characteristic of defective twitching behavior (Figure 3 lower panel).

Characterization of the EPS produced by *Xs* strains

As previously mentioned, EPS is a crucial virulence factor for different *Xanthomonas* spp.; therefore we studied the EPS production of the five strains. We observed that both Xs14 and Xs15 synthetized EPS (Figure 4); however none of the three *Xa* strains produced EPS (data not shown). We looked in the genomic sequence of *Xs* for the genes responsible of EPS synthesis; and checked the presence of the predicted *in silico* biosynthetic *gum* genes (*gumB*, *gumC*, *gumD*, *gumE*, *gumF*, *gumH*, *gumI*, *gumK*, *gumL*, *gumM*) by PCR and confirmed that Xs14 and Xs15 presented these genes (Figure S1a and S1b). It is worth noticing that, in both cases, amplicon fragment spanning from *gumF* to *gumH* sequences indicated the absence of the acetyltransferase coding *gumG* gene (Figure S1c), as the *in silico* prediction. We also observed that the EPS production of Xs14 and Xs15 was dependent on the addition of glucose to culture medium when the strains were grown in minimal defined medium salts (YMM) supplemented with glutamate as unique energy and carbon source (Figure S1d).

The production of EPS by Xs14 was significantly higher than the EPS production by Xs15 (Figure 4a); from here on, we will refer to them as EPS-Xs14 and EPS-Xs15. In contrast, both EPSs showed similar values of viscosity (LSRV) (Figure 4b). Moreover, while the macroscopic aspect of EPS-Xs14 and EPS-Xs15 was similar (Figure 4c), AFM analysis revealed microscopic differences in morphological features. Analysing the median value of height mean EPS strands

distribution as parameter, EPS-Xs15 (median value = 0.95 nm) presented strands with significantly higher mean height than EPS-Xs14 (median value = 0.61 nm) (Figure 4d and 4e). Because of the high degree of ramification of both EPSs, the contour length of the strands could not be measured.

A closer look at the chemical composition by CGL followed by MS analysis revealed that EPS-Xs14 and EPS-Xs15 consisted of the neutral monosaccharides glucose and mannose (Table 1). The presence of uronic acid was also detected in the samples (Table 1). In both cases, we observed no significant differences in molar and mass percentages between the EPSs. On the other hand, analytical determinations showed pyruvate and acetyl groups with significant differences in the degree of acetylation, being higher for EPS-Xs14 (Table 1).

Differences in cell adhesion and biofilm-like structures between *Xa* and *Xs* strains

Cell adhesion is involved in different steps of disease progression such as cell aggregation on the leaf surface and inner parts of the plant, and as a pre-requisite for biofilm formation (An *et al.*, 2019). We first assessed the ability of all five strains to attach to abiotic surface using the method developed by O'Toole and Kolter (1998). This *in vitro* bacterial adhesion assay revealed that *Xs* strains presented significantly higher cell adhesion than *Xa* strains (Figure 5a). In further experiments, we used CLSM to analyze whether the strains were able to form biofilm-like structures. In this assay, in agreement with the previous results, the three *Xa* strains failed to form defined biofilm structures and grew mostly like planktonic cells (Figure S2a); however, both *Xs* strains developed a mature biofilm after 72 h of incubation (Figure 5b). COMSTAT 2.1 analysis presented in Table 2 summarizes the differences in biofilm features among the strains. The roughness coefficient and diffusion distance were significantly higher for the biofilm formed by Xs15 when compared with the one formed by Xs14. These results indicated that Xs15 biofilm presented a more heterogeneous architecture, with variations in thickness, and less porous and confluent structure than Xs14 biofilm. It is important to highlight that Xs15 biofilm started to separate from the abiotic surface after 96 h of incubation (Figure 5b). In all cases, we confirmed that there were no major differences in growth between transformed strains used for CLSM analysis (Figure S2b and S2c).

Stomatal reopening as an invasion mechanism

Since preventing stomatal closure is a strategy for bacteria of the genus *Xanthomonas* to colonize the plant tissue (Melotto *et al.*, 2017), we wonder whether *Xa* and *Xs* strains presented a similar mechanism. To answer this question, we performed stomatal measurements using *Arabidopsis thaliana* epidermis. Figure 6a shows that after initial stomatal closure caused by bacterial MAMP perception, Xs14 and Xs15 were both able to reopen stomata. On the contrary, among *Xa* strains, only XaM6 was able to prevent stomatal closure, what brings out differences in *Xa* strains virulence factors battery.

In particular, the role of EPS-Xs as a suppressor of the stomatal closure was further analyzed. For that, we tested whether a pre-treatment of the epidermis with EPS-Xs14 or EPS-Xs15 could prevent a MAMP-induced stomatal closure triggered by flg22. As a positive control, xanthan extracted from *Xanthomonas campestris* pv. *campestris* (strain 8004) was used. In both cases, EPSs-Xs were able to significantly suppress flg22-induced stomatal closure, and the level of suppression was comparable to the positive control (Figure 6b).

DISCUSSION

In this work we found two *Xanthomonas* species associated with sugarcane leaf scald symptoms: *Xa*, the known causal agent of the disease and well-characterized pathogen and *Xs*, still an elusive pathogen; indeed, there are no reports describing *Xs* virulence factors and their role in plant disease. Here, we present a characterization of some pathogenic traits for both species. We described that, although there are some intraspecific variations, each species presented similar phenotypes for each factor analyzed. Interestingly *Xs* and *Xa* differ in key features related to disease progression and pathogenesis suggesting that these differences may define the niche that they occupied in the sugarcane plant.

We report differences in the epiphytic survival between *Xa* and *Xs* strains on sugarcane leaves. In particular, we think that *Xa* and *Xs* genetic traits help to explain this observation. In that sense, our results confirmed that *Xa* does not produce EPS *in vitro* in agreement with the absence of the *gum* operon in its genome (Pieretti *et al.*, 2012). As Mensi *et al*. (2016), we showed that *Xa* is able to adhere to inert surfaces, although very weakly compared to *Xs* strains. Taken together the lack of EPS matrix (not shown) and the weak cell adhesion (Figure 5a), we can explain why *Xa* strains failed to develop a mature biofilm (Figure S2a). Additionally, *Xa* strains were highly sensitive to oxidative stress. As mention before, different authors reported the role of xanthan and biofilm structures in protection from environmental stresses and epiphytic survival (Bütner and Bonas,

2010; Felipe *et al*., 2018). Consequently, we propose that the lack of EPS of *Xa* strains, their weak ability to adhere and to form biofilm as well as their high sensitivity to oxidative stress contribute, at least in part, to the lower epiphytic survival compare to *Xs*.

Furthermore, we showed that both strains of *Xs* present the biosynthetic xanthan *gum* genes in its genome and do produce a xanthan-like EPS. The presence of glucose, mannose, uronic acid as well as pyruvate and acetyl groups, in addition to the biosynthesis being dependent on the presence of a carbon substrate, indicated that EPS-Xs14 and EPS-Xs15 are in fact xanthan-like molecules. The EPS produced by *Xs* has not been described before. For this reason, the analysis of the chemical composition as well as rheological and spatial characteristics of this EPS could help us to understand its role in *Xs* biology. Consequently, we studied the degree of non-glucosyl substituents, since it depends on the *Xanthomonas* strain (Sutherland, 1981) and it can influence EPS conformation and properties such as viscosity (Hassler and Doherty, 1990). Although EPS-Xs14 presented more acetyl groups than EPS-Xs15, we observed no differences between the EPSs viscosity. This result can be explained by the similar proportion of acetyl:pyruvate between EPS-Xs14 and EPS-Xs15 (1:28 and 1:26 respectively). In addition, the absence of the acetyltransferase *gumG* suggests that the terminal mannose can only be pyruvilated, with no variation on the acetylation-pyruvilation grade depending on this residue. *In silico* studies showed that *gumG* is also missing in the *Xanthomonas translucens* genome (Charkhabi *et al.*, 2017). Interestingly both *Xs* and *X. translucens* belong to a reduced phylogenetic group (named group 1) along with *Xa*, *Xanthomonas hyacinthi*, *Xanthomonas theicola* (Young *et al.*, 2008). The absence of *gumG* might be a characteristic of some members of this group.

As we continued analyzing the EPS properties, we described that EPSs-Xs presented differences in the strands height. Variations in the number of aggregated strands can lead to differences in height (Ikeda *et al.*, 2012), as seen for EPSs-Xs. Indeed, EPSs with similar composition may differ in their structure having an impact on the functionality and characteristics of the matrix formed by the EPS (Kool *et al.*, 2013; Conforte *et al.*, 2019). In relation to this, both *Xs* strains developed biofilms with distinct characteristics. Xs14 formed a mature biofilm with a porous and homogenous structure, imbibed in an abundant EPS matrix. Moreover, the high EPS amount produced by Xs14 can explain a more adhesive biofilm phenotype. Taken this into account, although both *Xs* strains presented high tolerance to oxidative stress, and similar cell adhesion, we speculate that biofilm characteristics of Xs14 could result in bigger chances of survival on the phyllosphere.

When we analyzed cell motility, we found that *Xa* and *Xs* strains displayed particular and diverse phenotypes. Sliding and swimming differences seemed to correlate with the species, but not twitching variability. Sliding is a type of flagella-independent motility that depends on xanthan acting as a surfactant (Malamud *et al.*, 2011). According to this, sliding of *Xs* strains correlated with their EPS production. Similarly, *Xa* strains displayed very little sliding motility in agreement with the absence of a xanthan like molecule. As for *Xanthomonas citri* subsp. *citri*, *Xa* swimming responds to Rpf/DSF quorum-sensing regulation (Malamud *et al.*, 2011; Rott *et al.*, 2013). In particular for *Xa*, a low swimming phenotype may not impair infection, suggesting an important role for other motilities, like twitching, in sugarcane colonization (Rott *et al.*, 2013). For our strains, we could assume that the presence of an active flagellum and associated motility could be an advantage for *Xs* in the phyllosphere. However, further studies are needed to understand motility variations between strains and species.

Regarding the role of extracellular degradative, we propose that diversity between strains of *Xa* and *Xs* could be the result of different bacterial adaptations to certain plant niches. As it is suggested for *Xa* (Pieretti *et al.*, 2012), *Xs* could use endoglucanase for degradation of plant cell wall and obtaining a carbon source. Nevertheless, we did not detect amylase or protease activities produced by *Xa*. We could argue that *Xa* presents a different and more restrict battery of enzymes that we did not detect. A reduction in the enzyme activities of *Xa* may be expected since it lives mostly in the xylem, although with some contact with parenchyma cells (Mensi *et al.*, 2014). Based on this, we cannot rule out a role for protease and amylase activities. On the other hand, *Xs* could interact with living cells, spreading through apoplast and also xylem vessels. Note that *Xs* presented high tolerance to H_2O_2. This phenotype can be an advantage, along with the enzyme production, both in the epiphytic and endophytic phase of the pathogen.

In view of the suggested role of stomata in *Xa* disease cycle (Champoiseau *et al.*, 2009; Daugrois *et al.*, 2012) we studied the effect of *Xa* and *Xs* strains on stomatal movements. Our results indicated that both *Xs* strains were able to reopen stomata and this phenotype might be link to EPS acting as a suppressor of the plant response, as reported for xanthan of *X. campestris* pv. *campestris* (Bianco *et al.*, 2016). On the other hand, among *Xa* strains, only XaM6 was able to prevent stomatal closure, revealing variability between *Xa* strains. In this case a different molecule has to be involved in this regulation. It is well known that coronatine, a molecular mimic of Jasmonic Acid-Isoleucin, or syringolin A, a peptide toxin, both produced by pathovars of *Pseudomonas syringae* are involved in counteracting stomatal defense (Melotto *et al.*, 2017).

Similar scenarios have been reported in *Xanthomonas* spp., although how they facilitate stomatal reopening upon bacterial invasion is still unknown (Melotto *et al.*, 2017).

It is worth noting that, while Xa32 and Xa33 might enter the plant through naturally occurring or knives harvester produced wounds, XaM6 could also enter through stomata; *Xa* could have evolved different strategies for plant invasion. Furthermore, we could think that one strain could hitchhike the ability to open stomata from another without investing the resources, getting an evolutionary advantage. In a bigger picture, considering the richness and complexity of the phyllosphere (Remus-Emsermann and Vorholt, 2014), one could speculate that strains and/or species complement their strategies. Can the presence of a 'stomatal opener' improve the fitness of a pathogen that is not? Can the degradative activities of a pathogen help another one in the colonization of new niches? These questions, that require co-infection experiment, are however only fully meaningful if we used natural isolated pathogens

Finally, it is worth mentioning that both species were detected by PCR amplification using specific primers for leaf scald disease diagnosis (Pan *et al.*, 1999). Specificity of the primers was tested using several bacteria, including different *Xanthomonas* spp., although only one bacterium of group 1 (*X. translucens*) and not *Xs* (Pan *et al.*, 1999; Young *et al.*, 2008). Interestingly Ntambo *et al*. (2018) reported amplification with the same diagnostic primers when using *Xs* ACC10416 as a control. On the other hand, Lin *et al* (2018) could not amplify samples from plants with leaf scald symptoms using this and a different set of primers and hence suggested a *Xs* infection; all this highlight the difficulties and importance in developing specific diagnosis methods.

In conclusion, we studied virulence factors of *Xa* and *Xs* to gain insight into the biology of each microorganism. We recognized differences between the pathogen strategies that may influence the epiphytic survival and colonization mechanisms, helping us to understand in the future, the role of these two pathogens in sugarcane fields. Taken together, our results suggest that *Xa* and *Xs* colonize different parts of the sugarcane plant. We wonder which is the role of *Xs* in sugarcane fields in Argentina, as we showed that *Xs* have a battery of virulence factors typical for *Xanthomonas* spp., so it may be a sugarcane (or other plant) pathogen, as described by Sun *et al*. (2017). In this sense, as mentioned before, it is interesting to determine if *Xs* is associated to *Xa*, speculating that both species may act collaboratively or competitively. Another possible explanation is that *Xs* is not a native sugarcane pathogen and lives on the leaf surface of a non-host plant. *Xanthomonas arboricola* pv. *pruni* and *X. citri* subsp. *citri* can survive on non-host plants, and served as inoculum reservoir, having implications for plant disease epidemiology (Zarei *et al.*,

2018). The results presented here are a first step to understand both pathogens biology and their role in sugarcane diseases.

ACKNOWLEDGEMENTS

We thank Dr Francisco Velázquez for the critical reading of the manuscript and Dr Valeria P Conforte for her insightful comments and suggestions. We also thank the personnel of the EEAOC for the technical assistance. This work was supported by ANPCyT (PICT 2016-1586) and Project PIP-CONICET (grant number 112201501 00006CO).

DATA AVAILABILITY STATEMENT

The data that support the findings of this study are available from the corresponding author upon reasonable request.

REFERENCE

Aljanabi SM, Forget L, Dookun A, 1999. An Improved and Rapid Protocol for the Isolation of Polysaccharide- and Polyphenol-Free Sugarcane DNA. *Plant Molecular Biology Reporter* **17**, 281.

An SQ, Potnis N, Dow M *et al.*, 2019. Mechanistic insights into host adaptation, virulence and epidemiology of the phytopathogen *Xanthomonas*. *FEMS Microbiology Reviews* **44**, 1–32.

Becker A, Katzen F, Pühler A, Ielpi L, 1998. Xanthan gum biosynthesis and application: A biochemical/genetic perspective. *Applied Microbiology and Biotechnology* **50**, 145–152.

Bianco MI, Toum L, Yaryura PM *et al.*, 2016. Xanthan pyruvilation is essential for the virulence of *Xanthomonas campestris* pv. *campestris*. *Molecular Plant-Microbe Interactions* **29**, 688–699.

Büttner D, Bonas U, 2010. Regulation and secretion of *Xanthomonas* virulence factors. *FEMS Microbiology Reviews* **34**, 107–133.

Champoiseau P, Rott P, Daugrois JH, 2009. Epiphytic populations of X*anthomonas albilineans* and subsequent sugarcane stalk infection are linked to rainfall in Guadeloupe. *Plant Disease* **93**, 339–346.

Charkhabi NF, Booher NJ, Peng Z *et al.*, 2017. Complete genome sequencing and targeted mutagenesis reveal virulence contributions of Tal2 and Tal4b of *Xanthomonas translucens* pv. *undulosa* ICMP11055 in bacterial leaf streak of wheat. *Frontiers in Microbiology* **8**.

Conforte VP, Yaryura PM, Bianco MI *et al.*, 2019. Changes in the physico-chemical properties of the xanthan produced by *Xanthomonas citri* subsp. *citri* in grapefruit leaf extract. *Glycobiology* **29**, 269–278.

Daugrois JH, Rosiane Boisne-Noc, Champoiseau Patrice, Rott P, 2012. The Revisited Infection Cycle of *Xanthomonas albilineans*, the Causal Agent of Leaf Scald of Sugarcane. *Functional Plant Science and Biotechnology* **6**, 91–97.

Fang Y, Lin H, Wu L *et al.*, 2015. Genome sequence of *Xanthomonas sacchari* R1, a biocontrol bacterium isolated from the rice seed. *Journal of Biotechnology* **206**, 77–78.

Felipe V, Romero AM, Montecchia MS, Vojnov AA, Bianco MI, Yaryura PM, 2018. *Xanthomonas vesicatoria* virulence factors involved in early stages of bacterial spot development in tomato. *Plant Pathology* **67**, 1936–1943.

Filippone MP, Perera MF, Salgado M, García MG, Vellicce GR, Castagnaro A, 2010. Diagnóstico molecular de enfermedades sistémicas de la caña de azúcar en la Argentina: ajuste metodológico y aplicaciones. *Revista Industrial y Agricola de Tucumán* **87**, 01–11.

Filisetti-Cozzi TMCC, Carpita NC, 1991. Measurement of uronic acids without interference from neutral sugars. *Analytical Biochemistry* **197**.

Hassler RA, Doherty DH, 1990. Genetic Engineering of Polysaccharide Structure: Production of Variants of Xanthan Gum in Xanthomonas campestris. *Biotechnology Progress* **6**, 182–187.

Ikeda S, Gohtani S, Nishinari K, Zhong Q, 2012. Single Molecules and Networks of Xanthan Gum Probed by Atomic Force Microscopy. *Food Science and Technology Research* **18**, 741–745.

Kool MM, Gruppen H, Sworn G, Schols HA, 2013. Comparison of xanthans by the relative abundance of its six constituent repeating units. *Carbohydrate Polymers* **98**, 914–921.

Lane DJ, 1991. 16S/23S rRNA sequencing. In: *Nucleic acid techniques in bacterial systematics. E. Stackebrandt and M. Goodfellow, eds*. Chichester; New York: Wiley, 115–175.

Lin LH, Ntambo MS, Rott PC *et al.*, 2018. Molecular detection and prevalence of *Xanthomonas albilineans*, the causal agent of sugarcane leaf scald, in China. *Crop Protection* **109**.

Malamud F, Torres PS, Roeschlin R *et al.*, 2011. The *Xanthomonas axonopodis* pv. *citri* flagellum is required for mature biofilm and canker development. *Microbiology* **157**, 819–829.

Melotto M, Zhang L, Oblessuc PR, He SY, 2017. Stomatal defense a decade later. *Plant Physiology* **174**, 561–571.

Mensi I, Daugrois JH, Pieretti I *et al.*, 2016. Surface polysaccharides and quorum sensing are

involved in the attachment and survival of *Xanthomonas albilineans* on sugarcane leaves. *Molecular Plant Pathology* **17**.

Mensi I, Vernerey MS, Gargani D, Nicole M, Rott P, 2014. Breaking dogmas: The plant vascular pathogen *Xanthomonas albilineans* is able to invade non-vascular tissues despite its reduced genome. *Open Biology* **4**.

Noguera A, Paz N, Díaz ME *et al.*, 2014. Production of healthy seed cane in Tucumán, Argentina. *Revista Industrial y Agricola de Tucumán* **91**, 37–41.

Ntambo MS, Meng JY, Rott PC *et al.*, 2019. Identification and characterization of *Xanthomonas albilineans* causing sugarcane leaf scald in China using multilocus sequence analysis. *Plant Pathology* **68**.

O'Toole GA, Kolter R, 1998. Flagellar and twitching motility are necessary for Pseudomonas aeruginosa biofilm development. *Molecular Microbiology* **30**.

Pan YB, Grisham MP, Burner DM, Legendre BL, Wei Q, 1999. Development of polymerase chain reaction primers highly specific for *Xanthomonas albilineans*, the causal bacterium of sugarcane leaf scald disease. *Plant Disease* **83**, 218–222.

Pfeilmeier S, Caly DL, Malone JG, 2016. Bacterial pathogenesis of plants: future challenges from a microbial perspective: Challenges in Bacterial Molecular Plant Pathology. *Molecular plant pathology* **17**, 1298–1313.

Pieretti I, Cociancich S, Bolot S *et al.*, 2015. Full genome sequence analysis of two isolates reveals a novel xanthomonas species close to the sugarcane pathogen *Xanthomonas albilineans*. *Genes* **6**, 714–733.

Pieretti I, Royer M, Barbe V *et al.*, 2012. Genomic insights into strategies used by *Xanthomonas albilineans* with its reduced artillery to spread within sugarcane xylem vessels. *BMC Genomics* **13**, 658.

Remus-Emsermann MNP, Vorholt JA, 2014. Complexities of microbial life on leaf surfaces: The diversity of bacterial communities on leaves is comparable to that found in mammalian gastrointestinal tracts. *Microbe* **9**, 448–452.

Rott P, Fleites LA, Mensi I *et al.*, 2013. The RpfCG two-component system negatively regulates the colonization of sugar cane stalks by *Xanthomonas albilineans*. *Microbiology (United Kingdom)* **159**, 1149–1159.

Rott P, Davies M.J., 2000. Leaf Scald. In: *A Guide to Sugarcane Diseases* -. Montpelier: P. Rott, R. A. Bailey, J. C. Comstock, B. J. Croft and A. S. Saumtally, 38–44.

Studholme DJ, Wasukira A, Paszkiewicz K *et al.*, 2011. Draft genome sequences of *Xanthomonas sacchari* and two banana-associated xanthomonads reveal insights into the xanthomonas group 1 clade. *Genes* **2**, 1050–1065.

Sun HJ, Wei JJ, Li YS *et al.*, 2017a. First report of sugarcane leaf chlorotic streak disease caused by *Xanthomonas sacchari* in Guangxi, China. *Plant Disease* **101**.

Sutherland IW, 1981. Xanthomonas polysaccharides - Improved methods for their comparison. *Carbohydrate Polymers* **1**.

Young JM, Park DC, Shearman HM, Fargier E, 2008. A multilocus sequence analysis of the genus *Xanthomonas*. *Systematic and Applied Microbiology* **31**, 366–377.

Zarei S, Taghavi SM, Hamzehzarghani H, Osdaghi E, Lamichhane JR, 2018. Epiphytic growth of *Xanthomonas arboricola* and *Xanthomonas citri* on non-host plants. *Plant Pathology* **67**, 660–670.

Zhang HL, Ntambo MS, Rott PC *et al.*, 2020. Complete genome sequence reveals evolutionary and comparative genomic features of *Xanthomonas albilineans* causing sugarcane leaf scald. *Microorganisms* **8**.

SUPPORTING INFORMATION LEGENDS

Additional supporting information may be found online in the Supporting Information section.

Figure S1. *gum* operon and exopolysaccharide (EPS) production of *Xs*. (a) Scheme of *in silico* predicted *gum* operon organization. *gum* genes and locus tag are labeled. (b) Detection of biosyntethic genes (*gumB*, *gumC*, *gumD*, *gumE*, *gumF*, *gumH*, *gumI*, *gumK*, *gumL* and *gumM*) by PCR of genomic DNA of Xs14 and Xs15. (c) PCR amplification using *gumF*-FW1 and *gumH*-RV2 primers (arrows in the operon scheme). Amplicon size of 1.227 kb indicated the absence of *gumG* in the genomic DNA of Xs14 and Xs15 (arrow in the gel image). **(**d) EPS production of Xs14 and Xs15 grown for 48 h in Y minimal medium (YMM) with 0.11% (w/v) glutamate and with (+) and without (-) 1% (w/v) glucose.

Figure S2. Confocal laser scanning microscopy (CLSM) of *Xa* and growth curves of GFP-labeled strains. (a) CLSM images of *Xa* strains labeled with GFP after 48, 72 and 96 h of incubation. Bacterial growth curves in Y minimal medium (YMM) supplemented with 1% (w/v) sucrose, 0.11% (w/v) glutamate and 0.3% (w/v) cassaminoacids (n = 3; mean ± SEM) of Xs14 GFP-

labeled and Xs15 GFP-labeled (b) and Xa32 GFP-labeled, Xa33 GFP-labeled and XaM6 GFP-labeled (c).

Table 1S. Primers used in this work

FIGURE LEGENDS

Figure 1. Epiphytic survival of *Xa* and *Xs* on the phyllosphere. Bacterial growth on sugarcane leaves inoculated with cell suspensions of *Xs* strains (Xs14 and Xs15) (a) or *Xa* strains (Xa32, Xa33 and XaM6) (b). Cell population was assessed every two days from 0 up to 16 days post inoculation (dpi). The experiment was performed three times and two representative experiments are reported. Values are expressed as mean ± SEM from two independent experiments, each with triplicates. Grey arrows (8 dpi) indicate significant differences between Xs14 *vs.* Xa32 and XaM6; and Xs15 *vs.* XaM6. Black arrows (10 dpi) indicate significant differences between both Xs14 and Xs15 *vs.* Xa32, Xa33 and XaM6. Significant differences based on Tukey´s test (two-way ANOVA, $P < 0.0001$).

Figure 2. Sensitivity to oxidative stress and extracellular degradative enzyme production. (a) *Xa* and *Xs* sensitivity to different H_2O_2 concentrations. 100 mM H_2O_2: Xs14 and Xs15 area of growth inhibition not detectable below the threshold of the technic. One-way ANOVA showed no significant differences for Xa32, Xa33 and XaM6 data. 400 mM H_2O_2: different letters indicate significant differences based on Tukey´s test (one-way ANOVA, $P < 0.0001$). Each bar represents the mean and SEM from two independent experiments, each with four replicates. (b) Analysis of endoglucanase (left panel), protease (central panel) and amylase (right panel) activities. Bars represent the mean and SEM from three independent experiments, each one with triplicates. In the left panel, different letters indicate significant differences based on Tukey´s test (one-way ANOVA, $P < 0.0001$). In the central and left panel, asterisks indicate significant differences based on Student´s *t*-test (** and *** showing $P < 0.01$ and $P < 0.001$ respectively). ND: not detectable below the threshold of the technic.

Figure 3. Motility of *Xa* and *Xs* strains. Sliding (panel) and swimming (middle panel) motility measured as the colony outer halo of the growing bacterial cells (cm^2). Values are expressed as

mean ± SEM from three independent experiments, each one with triplicates. Different letters indicate significant differences based on Tukey´s test (one-way ANOVA, $P < 0.0001$) for both sliding and swimming analysis. Light microscopy of twitching halos (lower panel) from culture stained with crystal violet. Images were obtained using an inverted microscope at 40x magnification. Qualitative analysis indicates presence (+) or absence (-) of bacterial motility. Scale bars = 20 μm.

Figure 4. Analysis of exopolysaccharide (EPS) produced by Xs14 and Xs15 (EPS-Xs14 and EPS-Xs15 respectively). (a) EPS production determined as grams of dried EPS in relation to bacterial growth estimated as $\log_{10}$ (CFU/ml). Bars represent the mean and SEM from three experiments, each with duplicates. Asterisks indicate significant differences based on Student´s *t*-test (*** showing $P < 0.001$). (b) Low shear rate viscosity (LSRV) expressed as centipoise (cP). Data of four independent experiments is presented. Student´s *t*-test showed no significant differences between data. (c) Macroscopic appearance of EPS-Xs14 and EPS-Xs15 after ethanol precipitation. (d) Boxplot of the measured heights (H mean) of EPS strands. The sample sizes were EPS-Xs14 n = 29 and EPS-Xs15 n = 18. Asterisk indicates significant differences based on Mann-Whitney test (* showing $P < 0.05$). (e) Images of EPS strands observed by atomic force microscopy (AFM). Strand density/field is not representative. Images were taken randomly.

Figure 5. Cell adhesion and biofilm development. (a) Bacterial adhesion to an inert abiotic surface. Data represents the proportion of adhere to non-adhere bacteria (CV_{570}/OD_{600}). Bars represent the mean and SEM from three independent experiments, with 10 replicates each one. Different letters indicate significant differences based on Tukey´s test (one-way ANOVA, $P < 0.0001$). (b) Bacterial organization was analyzed using confocal laser scanning microscopy. Xs14 GFP-labeled (top) and Xs15 GFP-labeled (bottom) were grown in chambered cover slides, and images were taken at 48, 72 and 96 h. Square panels show the biofilm on the *x* and *y* planes, while bottom and right rectangles show the *z* plane. Scale bars represent 10 μm.

Figure 6. Stomatal aperture assays on *A. thaliana* epidermis. (a) Analysis of bacteria-induced stomatal closeure/aperture. Apertures were measured 1 and 3 h after incubation with bacterial suspensions. Asterisks indicate significant differences between stomata closure and reopening for each strain based on Sidak´s test (two-way ANOVA, **** and ** showing $P < 0.0001$ and $P <$

0.01 respectively). (b) Analysis of the effect of EPS in flg22-induced stomatal closure. Epidermial abaxial peels were incubated with xanthan from *X. campestris* pv. *campestris* 8004 (C+), a mock treatment performed with the 10:10 buffer (C-) or EPS-Xs, prior to incubation with flg22 to induce stomata closure. Different letters indicate significant differences based on Tukey´s test (two-way ANOVA, $P < 0.001$). In all cases, the aperture of 40 stomata was measured for each treatment per experiment. Data are presented as mean ± SEM of two independent experiments.

Table 1. Analysis of EPS composition

Sample	Glc (mol %)[a]	Man (mol %)[a]	Uronic acid (%)[b]	Pyruvate (%)[b]	Acetyl (%)[b]
EPS-Xs14	65.10 ± 6.98	30.04 ± 6.88	7.58 ± 1.73	0.47 ± 0.05	0.0170 ± 0.001 *
EPS-Xs15	62.54 ± 3.47	33.08 ± 3.66	7.04 ± 0.51	0.34 ± 0.04	0.0130 ± 0.001 *

Values represent mean ± SEM. Determinations were carried out in duplicate. Differences within a column were analyzed by Student´s *t*-test, means followed by asterisk are significantly different ($P < 0.05$).

[a] n = 4 for molar percentage of glucose (Glc) and mannose (Man). Molar percentage of trace elements (rhamnose and xylose) was approximately 5 % for both samples (data not shown).

[b] n = 3 for percentage of uronic acid, acetyl and pyruvate groups.

Table 2. Evaluation of biofilm properties by COMSTAT 2.1

Strain	Average thickness (μm)	Biomass ($\mu m^3/\mu m^2$)	Roughness coefficient (au)	Average Diffusion distance (au)
Xs14	18.63 ± 0.93	17.70 ± 0.96	0.09 ± 0.01 *	1.05 ± 0.10 *
Xs15	21.44 ± 1.08	19.71 ± 0.96	0.16 ± 0.02 *	1.40 ± 0.02 *

All data represent the mean ± SEM from two independent experiments; in a column, means followed by asterisk are significantly different ($P < 0.05$) according to Student´s *t*-test. Measurements of average thickness, biomass, roughness coefficient, average diffusion distance of 72 h-old biofilm.

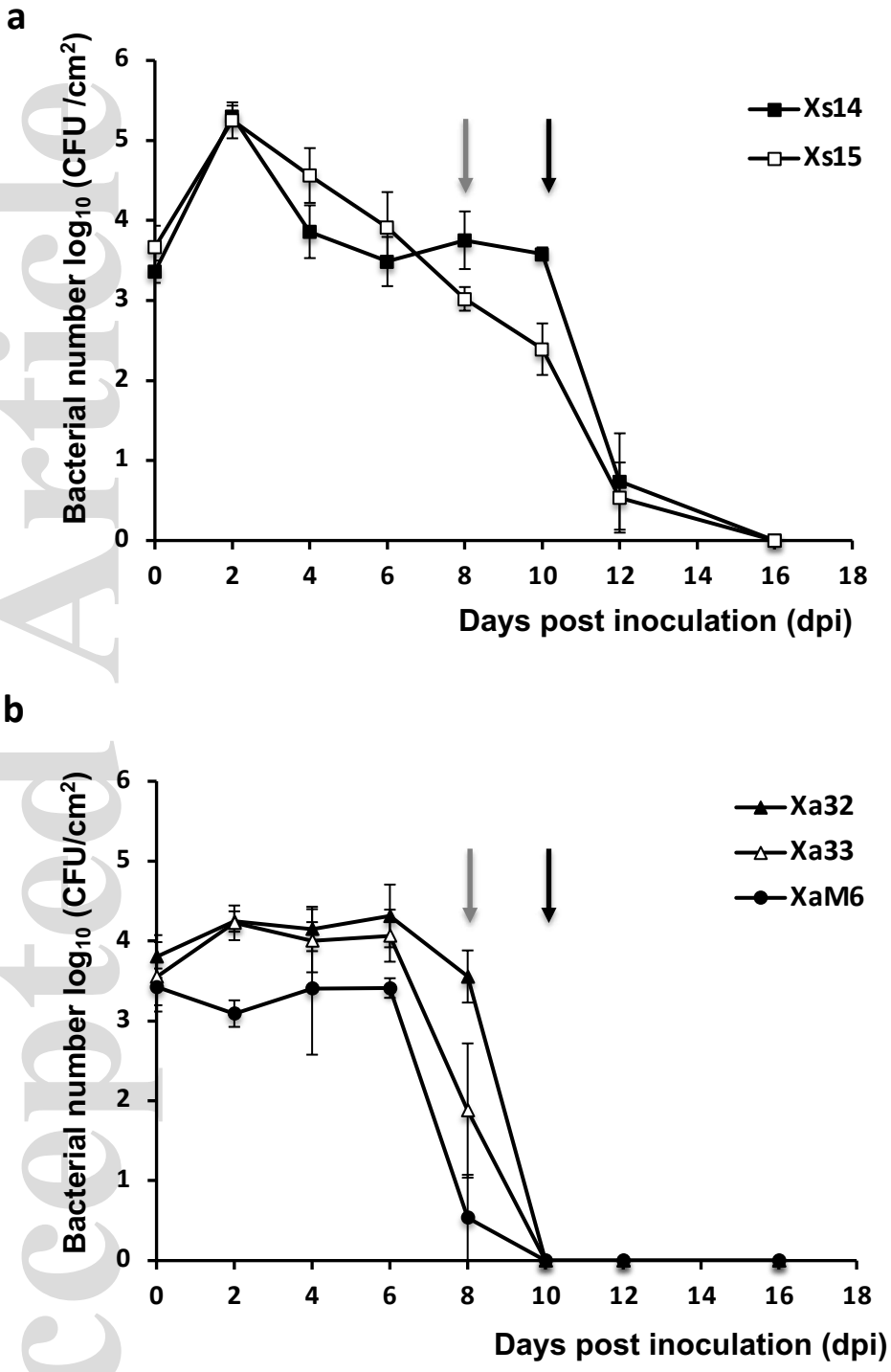

a

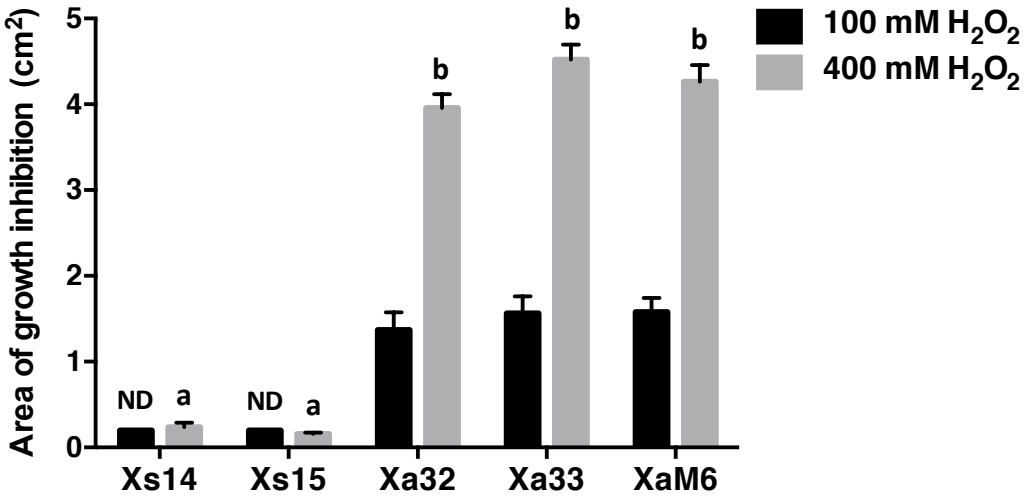

b

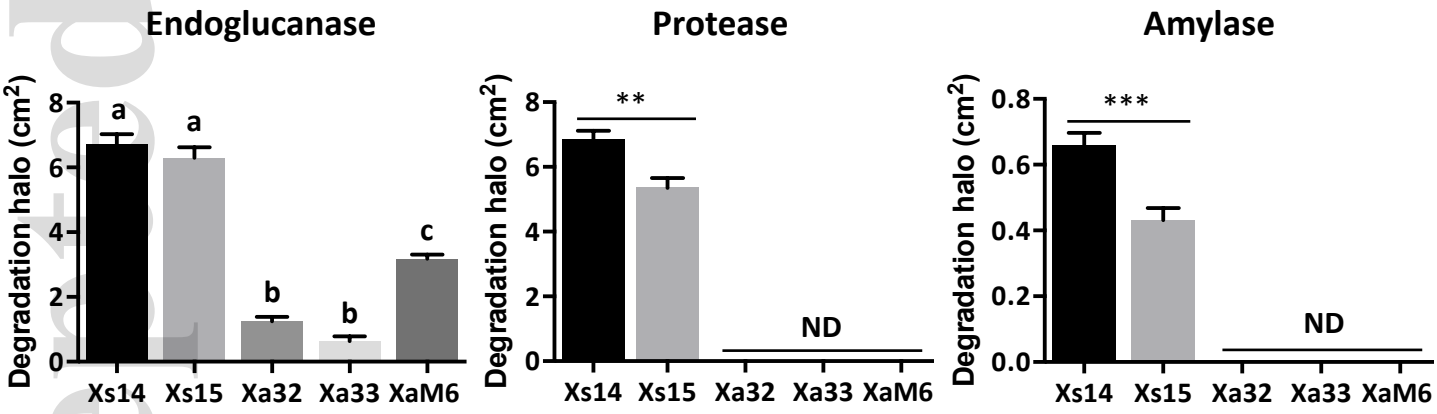

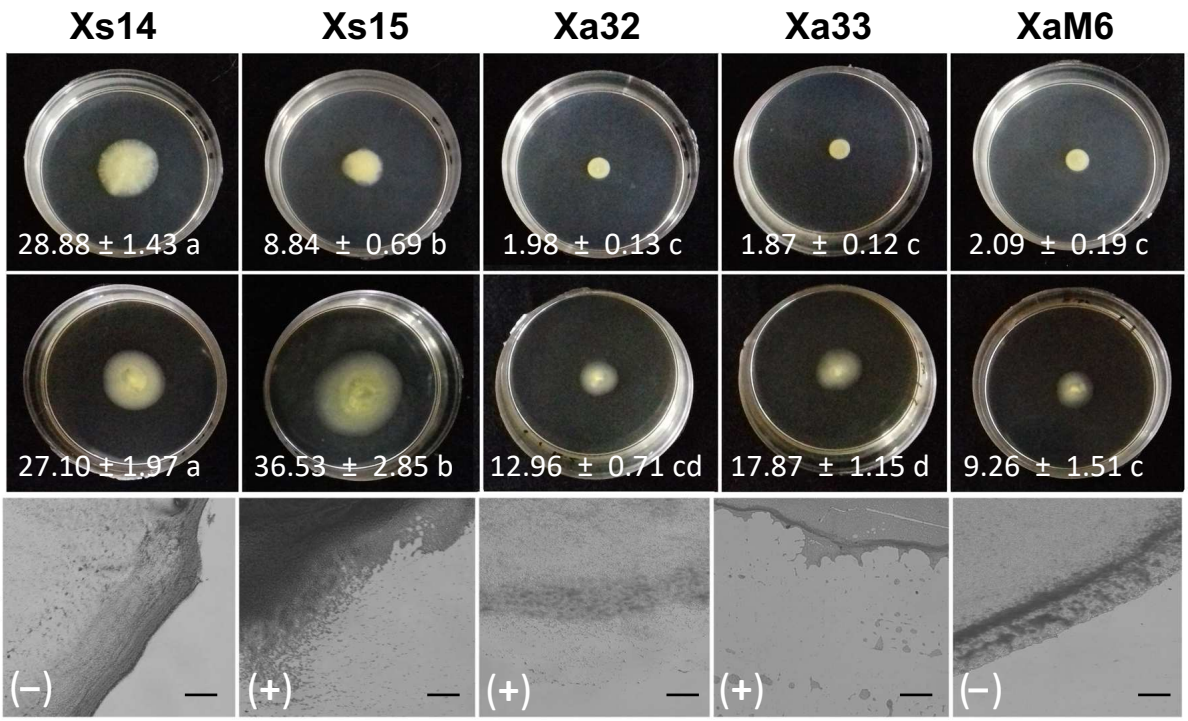

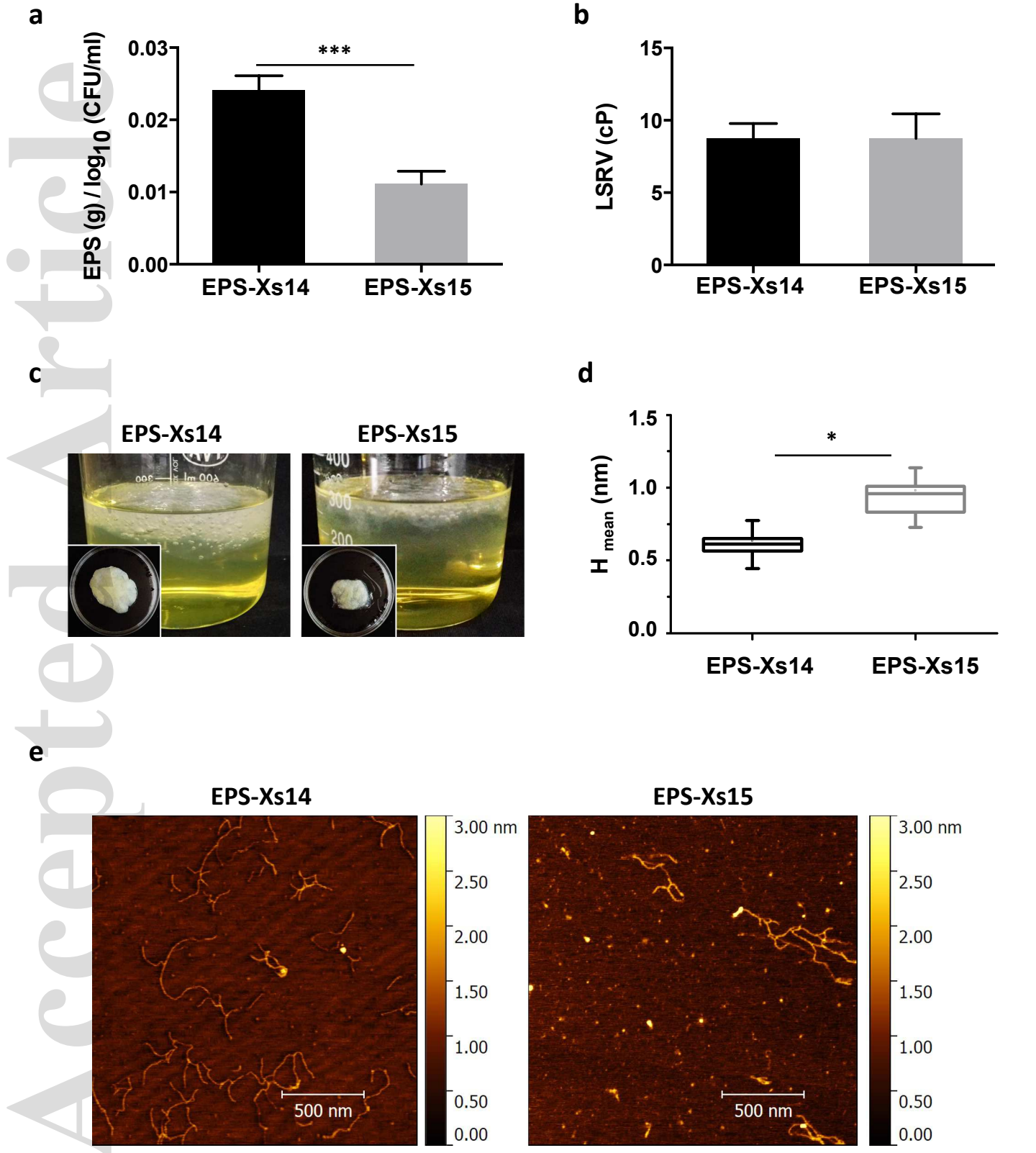

a

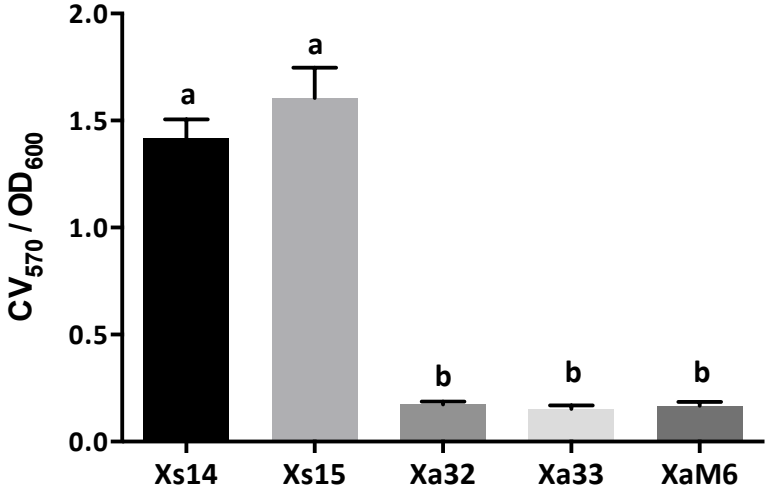

b

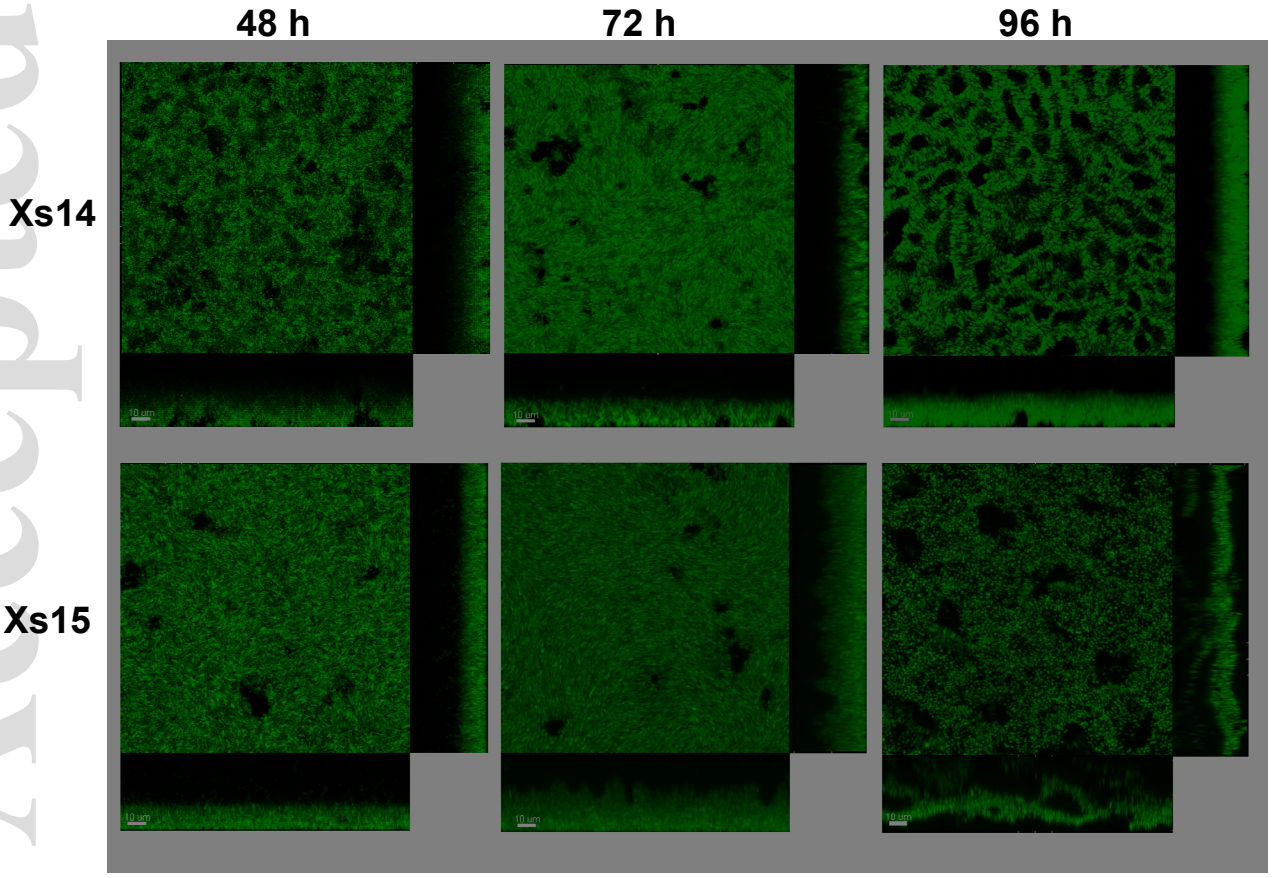

a

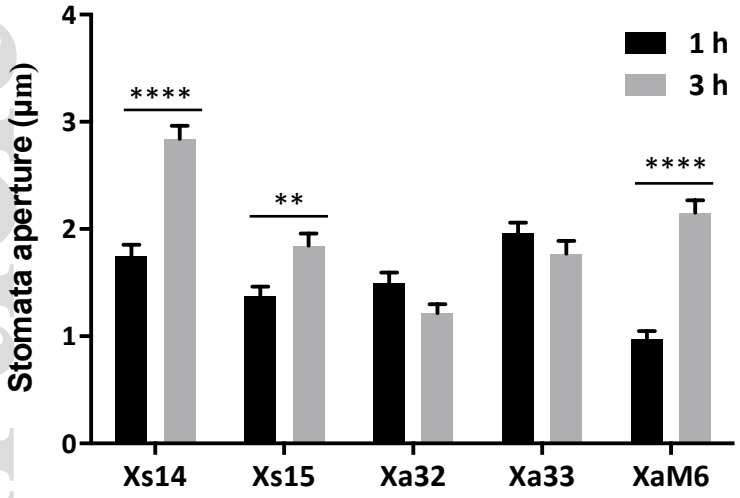

b